Fish and Shellfish Immunology 84 (2019) 312–321

Contents lists available at ScienceDirect

Fish and Shellfish Immunology

journal homepage: www.elsevier.com/locate/fsi

Full length article

Identification, characterisation and preliminary functional analysis of *IRAK-M* in grass carp (*Ctenopharyngodon idella*)

Pengfei Chu[a,b], Libo He[a], Denghui Zhu[a,b], Liangming Chen[a,b], Rong Huang[a], Lanjie Liao[a], Yongming Li[a], Zuoyan Zhu[a], Yaping Wang[a,*]

[a] State Key Laboratory of Freshwater Ecology and Biotechnology, Institute of Hydrobiology, Chinese Academy of Sciences, Wuhan, 430072, China
[b] University of Chinese Academy of Sciences, Beijing, 100049, China

ARTICLE INFO

Keywords:
Grass carp
IRAK-M
Innate immune
Subcellular localisation
MyD88

ABSTRACT

Interleukin-1 receptor-associated kinase (IRAK) family members play important roles in myeloid differentiation primary response 88 (MyD88)-dependent toll-like receptor (TLR) signaling, the crucial innate immune pathway in vertebrates. In the present study, the IRAK family gene *IRAK-M* (also called *IRAK3*) from grass carp (*Ctenopharyngodon idella*) was cloned and characterised. *IRAK-M* was mainly enriched in the spleen, and the significantly altered expression was observed after grass carp reovirus (GCRV) infection. Subcellular localisation showed that IRAK-M protein distributed uniformly in the entire cell and co-localised with MyD88 in the cytoplasm of transfected cells. Additionally, the interaction between IRAK-M and MyD88 was confirmed by bimolecular fluorescence complementation (BiFC) system. Moreover, deficient of IRAK-M in *C. idella* kidney cell line (CIK) with small interference RNA (siRNA) upregulated polyinosinic:polycytidylic acid (poly(I:C))-induced inflammatory cytokines production, including interleukin 8 (*IL-8*), *IL-6*, and tumour necrosis factor *α* (*TNF-α*), which reveals that IRAK-M functions as a negative regulator of inflammatory cytokines. Taken together, our results demonstrate that *IRAK-M* gene plays an important role in innate immune regulation and provide new insights into understanding the functional characteristics of the IRAK-M in teleosts.

1. Introduction

Interleukin (IL)-1 receptor-associated kinases (IRAK), which belongs to the serine/threonine protein kinase superfamily, contain a death domain that plays a crucial role in signaling cascades of the toll-like receptor (TLR) and interleukin-1 receptor (IL-1R) [1–3]. These signaling cascades are indispensable for elimination of viruses, bacteria, and cancer cells, as well as for wound healing [4]. In mammals, IRAK family consists of four members, IRAK1, IRAK2, IRAK-M (also called IRAK3), and IRAK4, which play important roles in both positively and negatively regulating the expression of inflammatory cytokines. All of four proteins contain an N-terminal death domain (DD), a ProST domain, and a central conserved kinase domain, but only IRAK1 and IRAK4 are active serine/threonine kinases [5]. By engaging MyD88 through their DD, IRAK1 and IRAK4 are able to interact with each other to initiate downstream signaling. IRAK4 is thought to autophosphorylate and then phosphorylate IRAK1 [6], which allows IRAK1 to initiate an autophosphorylation cascade occurring at several residues in the proST region in next sequential steps [7]. Unlike IRAK1 and IRAK4, IRAK2 cannot autophosphorylate, and it was initially thought to be a "pseudokinase" [8–11]. However, IRAK2 was detected to possess catalytic activity and had been implicated in maintenance of proinflammatory cytokine release [10]. Similar to other IRAK proteins, IRAK-M can form complexes with MyD88 and tumour necrosis factor (TNF) receptor associated factor 6 (TRAF6), but it is still considered as a pseudokinase because of limited capacity for autophosphorylation. However, the recent studies demonstrated that IRAK-M has potential to become activated and serve as a functional kinase [11].

Although with limited capacity for active kinases, IRAK-M is closely associated with many diseases, like sepsis [12,13], asthma [14,15], pneumonia [16,17], autoimmune diseases [18,19], and tumour [20]. Besides, following induced by TLR signaling, IRAK-M can express in response to various endogenous and exogenous soluble factors as well as cell surface and intracellular signaling molecules [21]. IRAK-M is known to be an important negative regulator in macrophages in models of inflammation. In mouse models of myocardial infarction, upregulation of IRAK-M in cardiac macrophages can reduce myocardial inflammation and prevent adverse cardiac remodeling [22]. Naïve monocytes and macrophages exposed to tumour cell lines exhibited reduced expression of tumour necrosis factor α (TNF-*α*), IL-12p40, and

* Corresponding author.
E-mail address: wangyp@ihb.ac.cn (Y. Wang).

https://doi.org/10.1016/j.fsi.2018.09.080
Received 5 July 2018; Received in revised form 28 August 2018; Accepted 29 September 2018
Available online 02 October 2018

IRAK1 [23,24]. IRAK-M–deficient (IRAK-M$^{-/-}$) nonobese diabetic (NOD) mice displayed early onset and rapid progression of Type 1 diabetes mellitus (T1DM) with impaired glucose tolerance, more severe insulitis, and increased serum anti-insulin autoantibodies. Moreover, IRAK-M$^{-/-}$ dendritic cells induced enhanced activation of diabetogenic T cells in vitro and the rapid onset of T1DM in *vivo* in immunodeficient NOD mice when cotransferred with diabetogenic T cells [25]. These data suggest that IRAK-M is a critical mediator of cross talk, however, the exact way of IRAK-M transcription regulation is largely unknown [4,21].

Interestingly, only three IRAK family members have been identified in fishes until now, IRAK1, IRAK-M and IRAK4 [26]. IRAK1 in *Gobiocypris rarus* [27], *Fenneropenaeus penicillatus* [28], *Epinephelus coioides* [1], and *Ctenopharyngodon idella* [29], IRAK4 in *Epinephelus coioides* [30], *Trachidermus fasciatus* [31], *Cynoglossus semilaevis* [32], and *Danio rerio* [33] were reported, while, the functions of IRAK-M are largely unknown in fishes. In the present study, *IRAK-M* gene from grass carp was cloned and characterised. Expression profiles in different tissues and in response to GCRV infection were examined in *vivo*. Additionally, the subcellular localisation of IRAK-M protein was investigated. Moreover, deficient of *IRAK-M* in grass carp kidney cell line (CIK) with small interference RNA (siRNA) was performed to investigate the possible roles of *IRAK-M*. These findings will provide new insights for understanding the functions of IRAK-M gene in teleosts.

2. Materials and methods

2.1. Experimental fish, plasmid, cells

Four-month-old healthy grass carps (weight, about 10 g; average length, 7 cm) were provided by the GuanQiao Experimental Station, Institute of Hydrobiology, Chinese Academic of Sciences, and acclimatized in aerated freshwater at 28 °C. The fish were fed twice a day with a commercial feed (Tong Wei, China). The pMN155 and pMC156 plasmids used in the study were a kind gift from Professor Zongqiang Cui, Wuhan Institute of Virology, Chinese Academy of Sciences and kept in our lab. The CIK cells (China Center for Type Culture Collection, China) used in the study were maintained in low glucose Dulbecco's modified Eagle's medium (DMEM; Hyclone, USA) supplemented with 10% fetal bovine serum and 1% (v/v) penicillin-streptomycin at 28 °C in a humidified atmosphere with 5% CO_2.

2.2. GCRV challenge and sample collection

Grass carps were acclimatized for 1 week and used for GCRV challenge experiment after no abnormal symptoms were observed. The GCRV preparation and GCRV challenge experiment were carried out as described previously [34].

Three uninfected fish were selected as the control group, and samples of the middle kidney, head kidney, liver, intestine, spleen, and gill were collected. Afterward, the tissues were also randomly sampled from three infected fish for six consecutive days after intraperitoneal injection. All samples were homogenized in TRIzol reagent (Invitrogen, USA) and stored at −80 °C prior to RNA extraction.

2.3. Cloning the full-length cDNA of IRAK-M

Total RNA was extracted from healthy samples by using TRIzol reagent, according to the manufacturer's instructions, and first-strand cDNA synthesis was performed using DNase I (Promega, USA) with total RNA as the template and random nonamer primers as the control for reverse transcriptase (Toyobo, Japan). The matched fragments of *IRAK-M* were obtained by blasting the homologous *IRAK-M* sequences (Accession no. BC098615.1) of zebrafish (*Danio rerio*) with draft genome of grass carp [35]. 5′ and 3′ untranslated regions (UTRs) of the *IRAK-M* gene were obtained by the rapid amplification of cDNA ends (RACE) PCR according to 5′ and 3′ Full RACE Kit (TaKaRa, Japan). The coding sequence (CDS) was amplified using PCR with primers within the 5′- and 3′-UTRs. The PCR products were purified, ligated into pMD18-T vectors (TaKaRa, Japan), and transformed into competent *Escherichia coli* DH5*α* cells (TransGen, China). Five positive colonies were selected and sequenced by a commercial company (Tsing Ke, China). The full-length cDNA of *IRAK-M* were obtained by comparing these PCR product sequences and discarding the obtained overlapping region sequence and vector sequence. The primers used for gene cloning and sequence verification were listed in Table S1.

2.4. Sequence analysis

BLAST (https://blast.ncbi.nlm.nih.gov/Blast.cgi) was used to search for the gene sequences in other species. Amino acid sequences of IRAK-M proteins were predicted using open reading frame (ORF) Finder (http://www.ncbi.nlm.nih.gov/projects/gorf/), and multiple sequence alignment was performed using ClustalW 2.1 (http://www.ebi.ac.uk/tools/clustalw2.1). SMART (http://smart.embl-heidelberg.de/) was used to predict the protein domain features. Tridimensional structure predictions of grass carp IRAK-M protein were performed using SWISS-MODEL (https://swissmodel.expasy.org/interactive/) and schematics were obtained using Swiss-PdbViewer 4.1 software. Neighbour-joining (NJ) phylogenetic trees were constructed on the basis of the amino acid sequences by using MEGA 7.0 software (http://www.megasoftware.net/index.html) and the bootstrap values of the branches were obtained by testing the tree 1000 times.

2.5. Tissue distribution of IRAK-M in grass carp

The total RNA was extracted from the tissues mentioned in 2.2 and then reverse-transcribed to obtain cDNA as described above. qRT-PCR and the CFX96™ real-time PCR detection system (Bio-Rad, USA) were used to measure the tissue distribution of *IRAK-M* in healthy grass carp. The housekeeping gene *β-actin* was used as a reference gene. Relative expression levels were calculated as the ratio of gene expression in each tissue relative to that in the middle kidney. The specific primers for qRT-PCR were listed in Table S1. Relative expression levels of *IRAK-M* were calculated using the $2^{-\triangle\triangle Ct}$ method [36]. All data were expressed as mean ± standard deviation (S.D.) values of three replicates.

2.6. Responses of IRAK-M to GCRV infection

Total RNA was extracted from six tissues (middle kidney, head kidney, liver, intestine, spleen, and gill) of three grass carp at different days after GCRV infection (1, 2, 3, 4, 5, and 6 days) and then reverse-transcribed to obtain cDNA as described above, which was used to examine the responses of *IRAK-M* to GCRV infection. The *β-actin* gene was used as a reference gene. Relative expression levels were calculated as the ratio of gene expression in the infected grass carps at each time point (1, 2, 3, 4, 5, and 6 days after GCRV infection) relative to that in the uninfected fish (0). Data were represented as mean ± S.D. values of three replicates. The significant difference ($p < 0.05$) between the control and treated groups at each time point was determined by Student's t-test.

2.7. Responses of IRAK-M and inflammatory cytokines in CIK cells after poly(I:C) stimulation

CIK cells seeded in six-well plates were stimulated with poly(I:C) (sigma, USA) at a final concentration of 20 μg/ml or phosphate-buffered saline (PBS) as control groups. Cells from each group were harvested at 3, 8, 24, 36, and 48 h post poly(I:C) stimulation. To further investigate the regulatory functions of *IRAK-M* gene in innate immunity, siRNA was performed to eliminate the expression of IRAK-M as following method. CIK cells seeded in six-well plates were transfected with siRNA by using

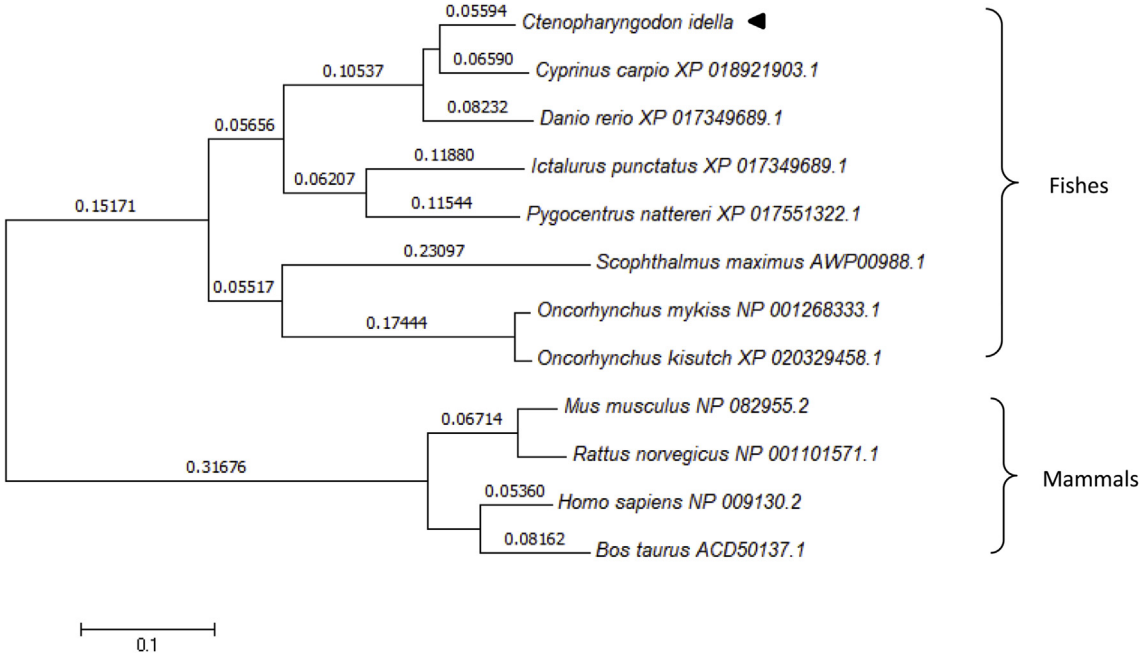

Fig. 1. Neighbour-joining phylogenetic tree analysis of IRAK-M. The tree was constructed based on amino acid sequences of grass carp IRAK-M and 11 orthologs using MEGA 7.0 software and the bootstrap values of the branches were obtained by testing the tree 1000 times.

the Lipofectamine™ 3000 Reagent (Imvitrogen, USA), according to the manufacturer's instructions. Firstly, the medium was renewed by 1.5 ml DMEM without fetal bovine serum and penicillin-streptomycin before transfection. Secondly, 5 μl Lipofectamine™ 3000 Reagent was diluted in 125 μl Opti-MEM™ Medium and 2.5 μg siRNA was diluted in 125 μl Opti-MEM™ Medium, then mixed them and incubated for 10 min at room temperature. Thirdly, the siRNA-lipid complex was added to cells gently and incubated for 12 h. Then the medium was renewed by DMEM supplemented with 10% FBS and 1% penicillin-streptomycin for another 12 h. After that poly(I:C) stimulation was carried out for 12 h, and then cells were harvested and total RNA was extracted and reverse transcribed to cDNA. The cDNA was used as a template for qRT-PCR to determine the expression levels of *IRAK-M* and inflammatory cytokines (*IL-8*, *IL-6*, and *TNF-α*). The specific primers for qRT-PCR and sequences of siRNA were listed in Table S1. Data were represented as mean ± S.D. values of three replicates. The significant difference ($p < 0.05$) between the control and treated groups at each time point was determined by Student's t-test.

2.8. Dual-luciferase activity assays

Plasmid pCMV-HA-IRAK-M was constructed as following method. Firstly, plasmid pCMV-HA was linearized with *EcoR*I and *Kpn* I (NEB, USA), and products were recovered by gel cutting and purification. Secondly, *IRAK-M* ORF from grass carp were amplified by specific primers (sequences were listed in Table S1) which were designed by CE Design (http://www.vazyme.com). Lastly, linearized pCMV-HA together with *IRAK-M* ORF was incubated at 37 °C for 30 min and then incubated on the ice straightway, according to the manufacturer's instructions of ClonExpress kit (Vazyme, USA). Sequences of the resulting plasmids were verified by DNA sequencing.

CIK cells were seeded in each well of 24-well plate with 300 μl DMEM before transfection and incubated at 28 °C overnight. Subsequently, the cells were transfected by the mixture containing 200 ng of pNF-κB-TALuc (Beyotime, Jiangsu, China) that carries four tandem copies of the NF-κB binding consensus sequence (GGGAATT TCC) fused to a pTA promoter, 300 ng of pCMV-HA-IRAK-M or empty vector (pCMV-HA, Clontech, USA), 5 ng of pRL-TK Renilla plasmid (Promega) and 1 μl of Lipofectamine 3000 (Invitrogen) as the method described above. Then cells were lysed by 100 ml of 1× Passive Lysis Buffer (Promega) and luciferase activities were detected by using a Dual-Luciferase Reporter Assay System (Promega). Data were represented as mean ± S.D. values of three replicates. The significant difference ($p < 0.05$) between the control and treated groups at each time point was determined by Student's t-test.

2.9. Subcellular localisation of IRAK-M and related proteins

To analyse the subcellular localisation of IRAK-M, IRAK-M-pDsRed vector was constructed as the method described above. The day before transfection, CIK cells were plated evenly in six-well plates with glass bottoms for 24 h to 70–80% confluence. Then, the vectors were transiently transfected into the CIK cells as the method described above. At 24 h post-transfection, the cells were fixed with 4% paraformaldehyde, permeabilized with 0.2% Triton X-100, and stained with Hoechst 33342 (Beyotime, China). The CIK cells were observed using the UltraVIEW VOX confocal system (PerkinElmer, Fremont, CA, USA) and a 63 × oil immersion objective lens.

To further investigate the relationship between IRAK-M and related proteins, TRAF6-pEGFP, IRAK1-pEGFP, and MyD88-pEGFP vectors were constructed as the method described above. Then, the EGFP-tag plasmids were transfected into CIK cells together with IRAK-M-pDsRed, respectively as described above.

2.10. Validation of the interaction between IRAK-M and related proteins

TLRs play crucial roles for host to recognize and defense against pathogens in fishes [37]. IRAK proteins have been identified as fatal regulators involved in TLRs signaling pathways via binding or dissociating with MyD88 and TRAF6 in mammals in recent years. In order to further understand the functions of IRAK-M protein, the bimolecular fluorescence complementation (BiFC) system was introduced to detect whether IRAK-M could interact with TRAF6, IRAK1, and MyD88. Briefly, the ORF sequences of TRAF6, IRAK1, MyD88, and IRAK-M (amplified by the primers listed in Table S2) were cloned from grass carp and inserted into the pMN155 and pMC156 plasmids, respectively. The final plasmids were named pTRAF6-MN155, pIRAK1-MN155, pMyD88-MN155, and pMC156-IRAK-M, which contained the N-

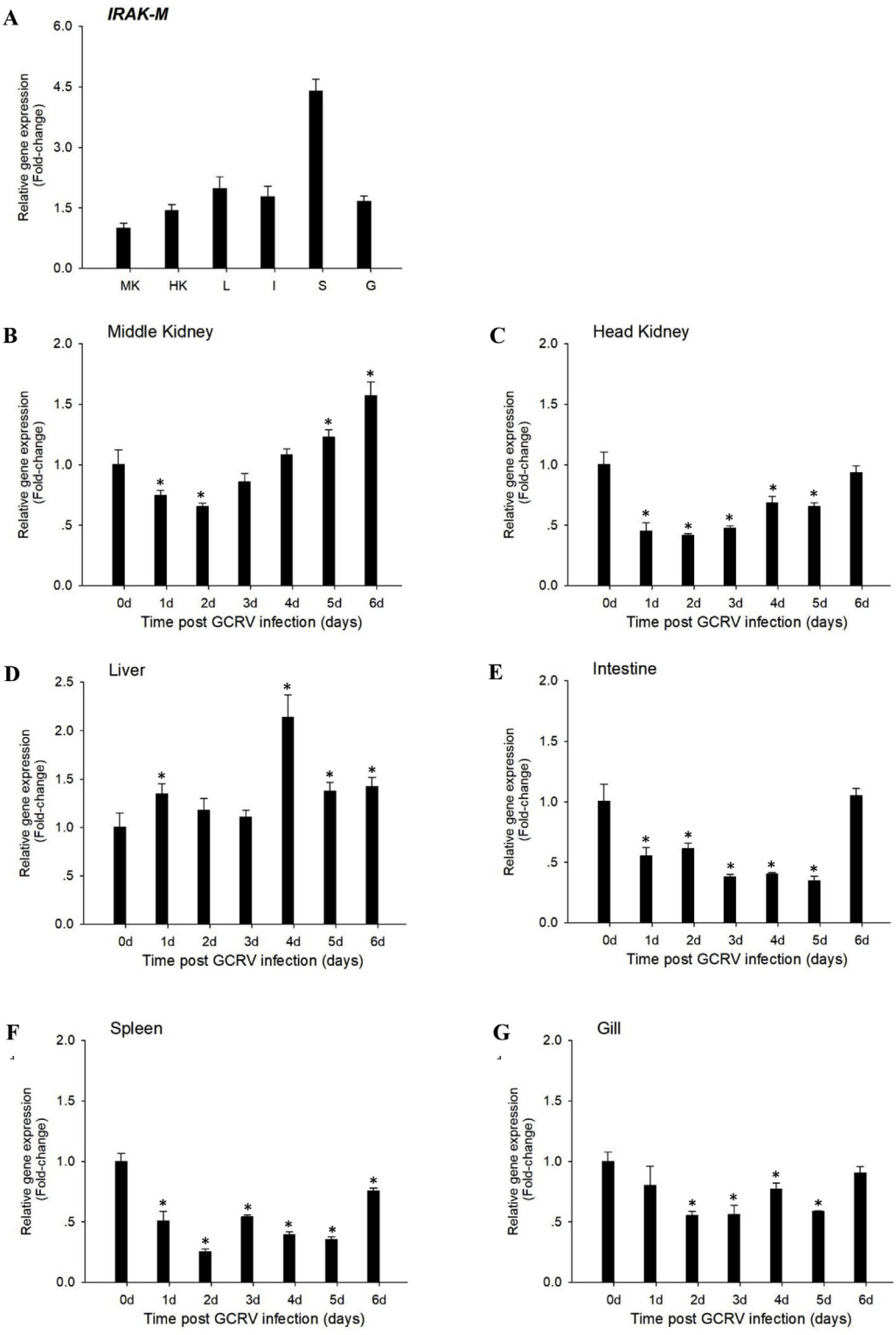

Fig. 2. Tissue distribution of *IRAK-M* and expression pattern following GCRV infection. RNA was isolated from the middle kidney (MK), head kidney (HK), liver (L), intestine (I), spleen (S), and gill (G) and subjected to qRT-PCR analysis. A. Relative expression levels of *IRAK-M* were calculated on the basis of the ratio of gene expression in the different tissues relative to that in the middle kidney. The expression levels of *β-actin* were used as an internal control. B-G. Expression levels of *IRAK-M* in the healthy group (day 0) were set to 1. *β-actin* was used as an internal control to normalize the relative expression levels of the target genes. The results were based on three independent experiments and expressed as mean ± standard deviation (S.D.) values. Significant difference ($p < 0.05$) between the control and treated group was indicated with asterisks (*).

terminal of mNeptune (mNeptune aa 1–155, MN155) and C-terminal of mNeptune (mNeptune aa 156C-terminal, MC156), respectively. Then, plasmids pTRAF6-MN155, pIRAK1-MN155, and pMyD88-MN155 were transfected into CIK cells alone or together with pMC156-IRAK-M as described above. At 24 h post-transfection, the cells were fixed with 4% paraformaldehyde, permeabilized with 0.2% Triton X-100, and stained with Hoechst 33342 (Beyotime, China). The CIK cells were observed using the UltraVIEW VOX confocal system (PerkinElmer, Fremont, CA, USA) and a 63 × oil immersion objective lens.

3. Results

3.1. Molecular characterisation and phylogenetic analysis of IRAK-M

The full length cDNA of *IRAK-M* (Genbank accession number: MH590729) is 2172 bp long, with a 1851 bp ORF encoding a predicted polypeptide of 616 amino acids, 144 bp 5′ UTR, and 177 bp 3′ UTR. The SWISS-MODEL was used to predict the tertiary structure of grass carp IRAK-M proteins, and the SPDBV software was used to display the

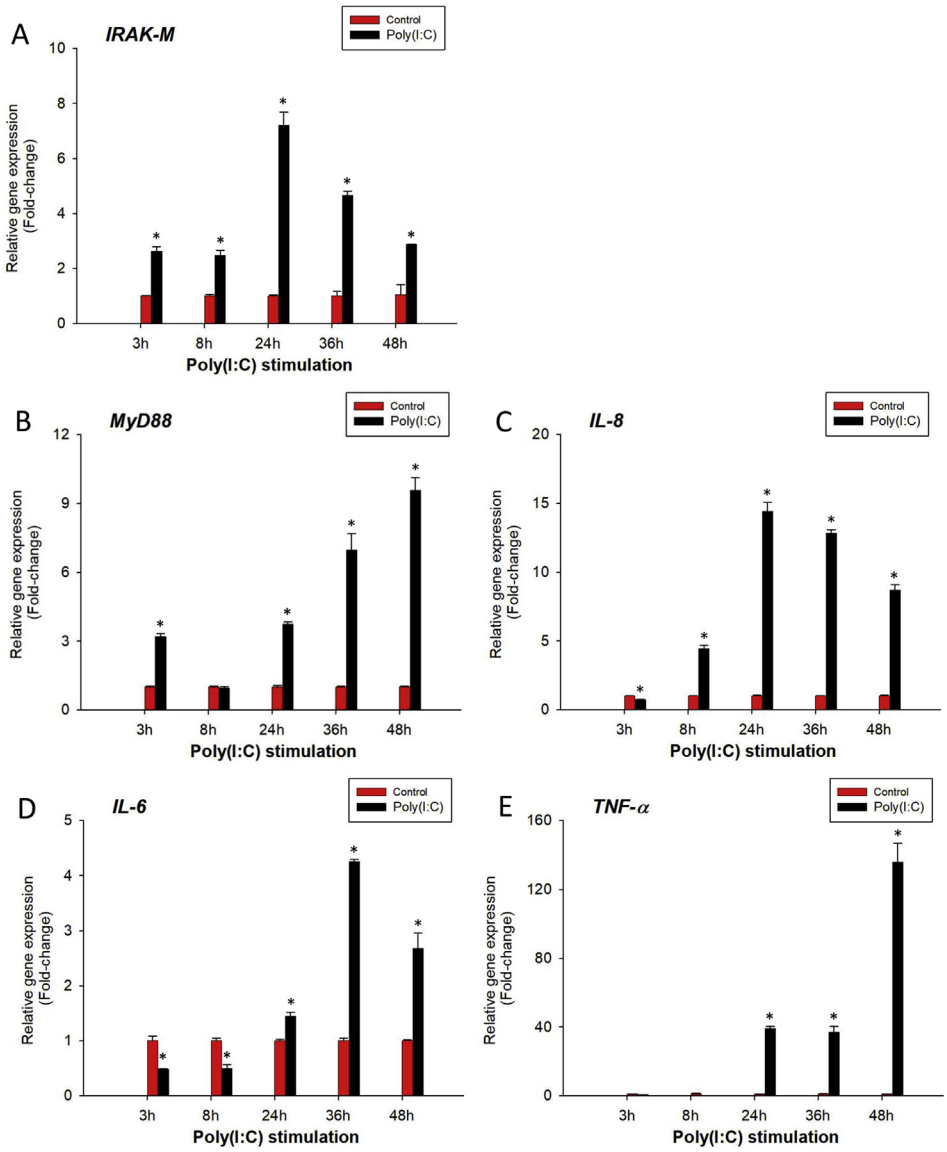

Fig. 3. Analysis of *IRAK-M* and related gene expression after poly(I:C) stimulation. RNA was isolated from each cells group (3, 8, 24, 36, and 48 h post poly(I:C) stimulation) subjected to qRT-PCR analysis. Expression levels of these genes in the PBS group at each point were set to 1. *β-actin* was used as an internal control to normalize the relative expression levels of the target genes. The results were based on three independent experiments and expressed as mean ± standard deviation (S.D.) values. Significant difference ($p < 0.05$) between the control and treated group was indicated with asterisks (*).

predicted tertiary structure diagram. As showed in Fig. S1, IRAK-M protein contained typical *α*-helices and *β*-sheets. Structure analysis revealed that IRAK-M consists of a conserved kinase domain (KD, aa 156–433) flanked by an N-terminal DD domain (aa 20–99) involved in binding to other IRAK family members [11]. Sequence alignment showed that the DD domain and KD domain were both well conserved in fishes. Besides, compared to mammalian IRAK-M, a C-terminal domain of Leucine-rich repeat (LRR, aa 559–587) was predicted in grass carp IRAK-M protein. Evolutionary relationship analysis based on the full-length amino acid sequences of IRAK-M in other species revealed that IRAK-M could be classified into two groups: IRAK-M proteins from the fishes fell into one branch; IRAK-M proteins from mammals fell into another branch. IRAK-M from grass carp was closely related to that of *C. carpio*, and *D.rerio*. (Fig. 1).

3.2. Tissue distribution of IRAK-M in healthy grass carp

Six tissue samples (middle kidney (MK), head kidney (HK), liver (L), intestine (I), spleen (S), and gill (G)) were isolated from three healthy grass carps for qRT-PCR to analyse the tissue distribution of the *IRAK-M* gene in grass carp. As shown in Fig. 2A, *IRAK-M* was mainly enriched in the spleen and far more than the second high expression levels in the liver. *IRAK-M* expressed the lowest in the middle kidney.

3.3. Analysis of IRAK-M expression following GCRV infection

To determine whether *IRAK-M* is involved in the innate immune responses to GCRV infection, a viral challenge experiment was performed and samples were collected for qRT-PCR analysis.

Following GCRV stimulation, *IRAK-M* mRNA expression levels were altered in all the detected tissues. In the liver, *IRAK-M* were upregulated on day 1, subsequently, slightly reduced, then sharply upregulated again and peaked on day 4, afterward decreased at the late stage. In the middle kidney, *IRAK-M* were downregulated on the first two days after GCRV infection, then, increased steadily and reached the peak on the day 6. *IRAK-M* mRNA expression levels were suppressed significantly during all the detected time in the other tissues (Fig. 2B–G).

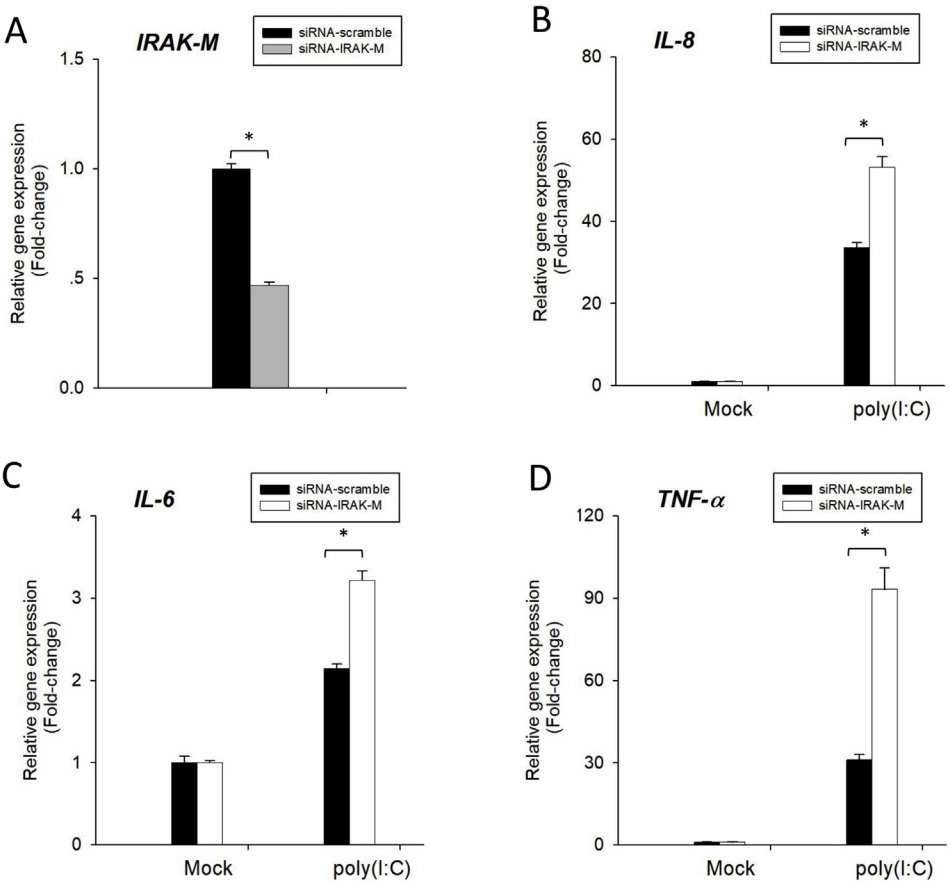

Fig. 4. Functional analysis of IRAK-M in CIK cells. IRAK-M deficient CIK cells were generated with siRNA. RNA was isolated from each treated cells group and subjected to qRT-PCR analysis. The expression levels of these genes in the control group were set to 1. *β-actin* was used as an internal control to normalize the relative expression levels of the target genes. The results were based on three independent experiments and expressed as mean ± standard deviation (S.D.) values. Significant difference ($p < 0.05$) between the control and treated group was indicated with asterisks (*).

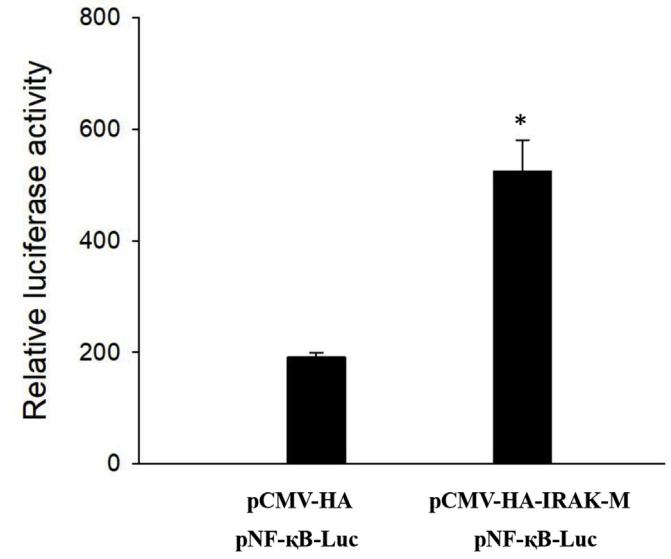

Fig. 5. Activation of the promoter activity of NF-κB by IRAK-M. NF-κB activity is monitored by a pNF-κB-TA-Luc reporter system in CIK cells co-transfected with pCMV-HA-IRAK-M or empty vector (pCMV-HA). Renilla luciferase activity was detected as the internal control and relative luciferase activity levels were expressed as fold increase of luciferase activity. The results were based on three independent experiments and expressed as mean ± standard deviation (S.D.) values. Significant difference ($p < 0.05$) between the control and treated group was indicated with asterisks (*).

3.4. Functional analysis of IRAK-M in CIK cells

In order to explore the functions of IRAK-M during innate immunity, the mRNA expression levels of *IRAK-M*, *IL-8*, *MyD88*, *IL-6* and *TNF-α* were detected after poly(I:C) stimulation in CIK cells. As shown in Fig. 3, compared with the control, the expression levels of *IRAK-M*, *IL-8*, *MyD88*, *IL-6*, and *TNF-α* were significantly upregulated following poly (I:C) stimulation.

To further assess the regulatory effects of IRAK-M on innate immune regulation, IRAK-M deficient CIK cells were generated using siRNA (Fig. 4A), and expression levels of *IL-8*, *IL-6*, and *TNF-α* were investigated after poly(I:C) stimulation in deficient CIK cells. As shown in Fig. 4, compared to the controls, expression of *IL-8*, *IL-6*, and *TNF-α* were all significantly heightened. Taken together, these results suggest that IRAK-M is a negative regulator of inflammatory cytokines.

3.5. Activation of the promoter activity of NF-κB by IRAK-M

To analyse the role of grass carp IRAK-M in NF-κB signal path, further experiments were performed. The plasmids pCMV-HA-IRAK-M and pNF-κB-Luc were co-transfected into CIK cells for 24 h, and then the NF-κB activity was detected by luciferase activity assay. As shown in Fig. 5, the results showed that IRAK-M up-regulated the promoter activity of NF-κB.

3.6. Subcellular localisation of IRAK-M and related proteins

To investigate the subcellular localisation of the IRAK-M protein, CIK cells were transfected with IRAK-M-pDsRed plasmids, and then fluorescence was observed at 24 h post-transfection. The empty pDsRed2-C1 plasmids were also transfected at the same time as the negative control. IRAK-M-pDsRed was strongly distributed uniformly

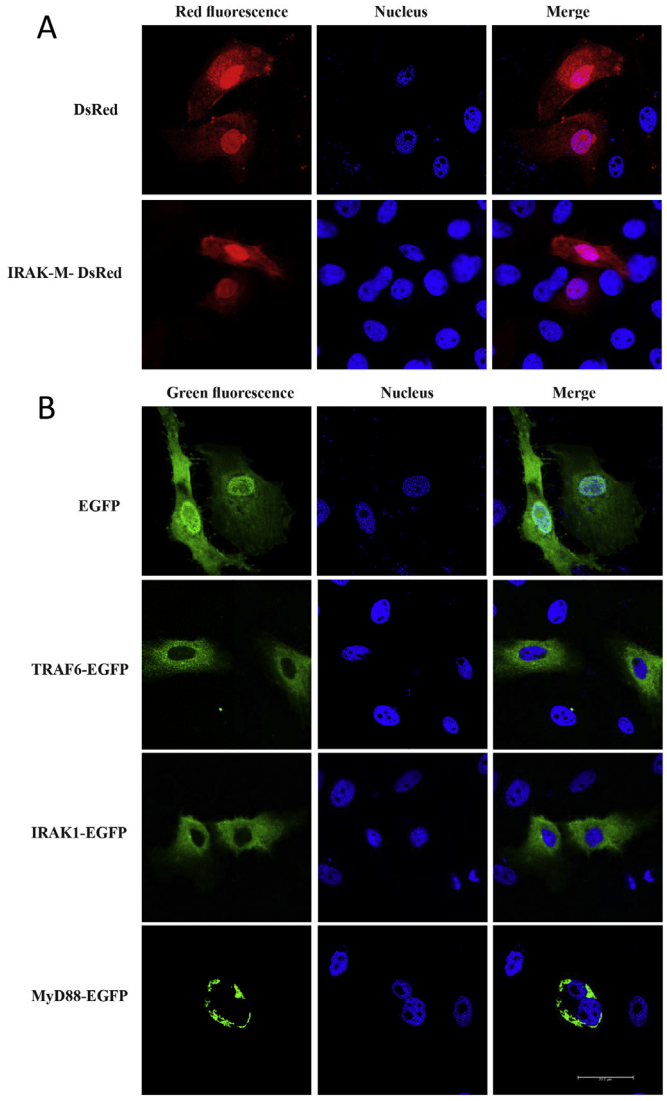

Fig. 6. Subcellular localisation of IRAK-M and related gene in CIK cells. Cells were transfected with the plasmids (IRAK-M-pDsRed, TRAF6-pEGFP, IRAK1-pEGFP, MyD88-pEGFP), and fluorescence was observed at 24 h post-transfection. Red/Green fluorescence showed the distribution of pDsRed/EGFP-tagged proteins, and blue fluorescence showed the nucleus stained with Hoechst 33342 under a 63 × oil immersion objective lens (scale bar, 20 μm). (For interpretation of the references to colour in this figure legend, the reader is referred to the Web version of this article.)

throughout the entire cell, the same as pDsRed2-C1 (Fig. 6A). In order to exclude the false positive results caused by the degradation of IRAK-M protein, IRAK-M-pEGFP was also constructed and transfected into CIK cells, the results showed the same pattern with IRAK-M-pDsRed (Fig. S3).

Further, the relationship between IRAK-M and related proteins was investigated by subcellular localisation. Firstly, TRAF6-pEGFP, IRAK1-pEGFP, and MyD88-pEGFP were transfected into CIK cells alone, respectively. As shown in Fig. 6B, TRAF6 and IRAK1 were strongly distributed uniformly in the cytoplasm, while MyD88 was presented as spot and only observed in the cytoplasm surrounding the cell nucleus. Moreover, the EGFP-tag plasmids were transfected into CIK cells together with IRAK-M-pDsRed, respectively. As shown in Fig. 7, no or only little co-loclisation was observed between TRAF6 or IPAK1 and IPAK-M. However, when cotransfection of IRAK-M-pDsRed and MyD88-pEGFP, a remarkably bright signal occurred in the colocalisation of IRAK-M and MyD88, suggesting that MyD88 could recruit and relocate IRAK-M protein.

3.7. Interaction between IRAK-M and MyD88

In the present study, the mNeptune-based BiFC system was used to visualize the interaction of TRAF6, IRAK1, and MyD88 with IRAK-M in living cells. When pTRAF6-MN155 and pIRAK1-MN155 were transfected into CIK cells alone or together with pMC156-IRAK-M, no fluorescence signal was observed (data not shown). However, co-transfection of pMyD88-MN155 and pMC156-IRAK-M resulted in a bright red mNeptune fluorescence signal in the cytoplasm surrounding the cell nucleus (Fig. 8). The bright red mNeptune fluorescence signal was not observed when it came to transfection of pMyD88-MN155 or pMC156-IRAK-M alone. Thus, the results further confirmed that IRAK-M interacted with MyD88 in CIK cells.

4. Discussion

TLRs family plays an important role in the innate immunity of vertebrate and invertebrate by recognizing a series of highly conserved pathogenic microorganism structures, termed pathogen-associated molecular patterns (PAMPs) [38,39]. The signaling pathway of TLRs are MyD88-dependent (except TLR3) and could induce inflammatory-cytokine production via nuclear factor-κB (NF-κB) activation. IRAKs family is known as a regulator in signaling cascades of the TLR. In mammals, the N-terminal DD of IRAK proteins could form a signal transduction complex with MyD88, maintain interactions with downstream proteins such as TRAF6 to initiate signaling, in which IRAK1 was phosphorylated and activated by autophosphorylated IRAK4 [6]. Then, activated IRAK1 dissociates from the MyD88 complex and associates with TRAF6, facilitating the activation of NF-κB [4]. IRAK1, IRAK2, and IRAK4 play positive roles while IRAK-M acts as a negative regulator in this signaling pathway. Interestingly, no IRAK2 protein has yet been identified in any fish species, and our results also support the notion that teleost IRAK separated into IRAK-1, M and 4 before the separation of IRAK-2, implying that the IRAK family members may have not diverged fully in the lower vertebrates [26], and function as a little different roles with mammals. In the present study, *IRAK-M* gene was identified in grass carp and investigated. In vertebrates, the N-terminal death domain (DD) of IRAK family is conserved in a wide range of species. In the study, a DD domain (aa 19–95) in the N-terminal and catalytic domain (aa 162–437) in the central were also predicted. Phylogenetic analysis and multiple sequence alignments analysis revealed that IRAK-M from grass carp showed the closest relationship and high homology (85%) with the homologues from *C. carpio*, while low homology (35%) with human, its well conserved cDNA sequence in teleost indicates IRAK-M is likely to be ancestral needs.

In contrast to other human IRAK members, whose expression are ubiquitous, the expression of IRAK-M is predominantly in the spleen and lung, and limited mostly to cells of the monocytic lineage [11]. Murine IRAK-M has been shown to be expressed in many cell types occurring most predominantly in the liver and thymus [40]. In the present study, grass carp IRAK-M was mainly detected in the spleen which is the main innate immune tissue in teleost, suggesting an important immune function of IRAK-M. To our surprise, IRAK-M mRNA expression levels were suppressed significantly during all the detected time except that in the liver and the middle kidney after GCRV stimulation (Fig. 2). Besides, Remarkable fluctuation of IRAK-M in response to GCRV infection in the liver and the middle kidney was also observed (Fig. 2), which indicated IRAK-M plays an important role in innate immunity. RNAi in CIK cells is an effective way to analysis gene function in *vivo* [41,42]. In the present study, IRAK-M deficient CIK cells were generated to assess the regulatory effects of *IRAK-M* on innate immune responses. As shown in Fig. 4, the significantly heightened expression of *IL-8*, *IL-6* and *TNF-α* after poly(I:C) stimulation in IRAK-M deficient CIK cells suggested that IRAK-M acts as a negative regulator of

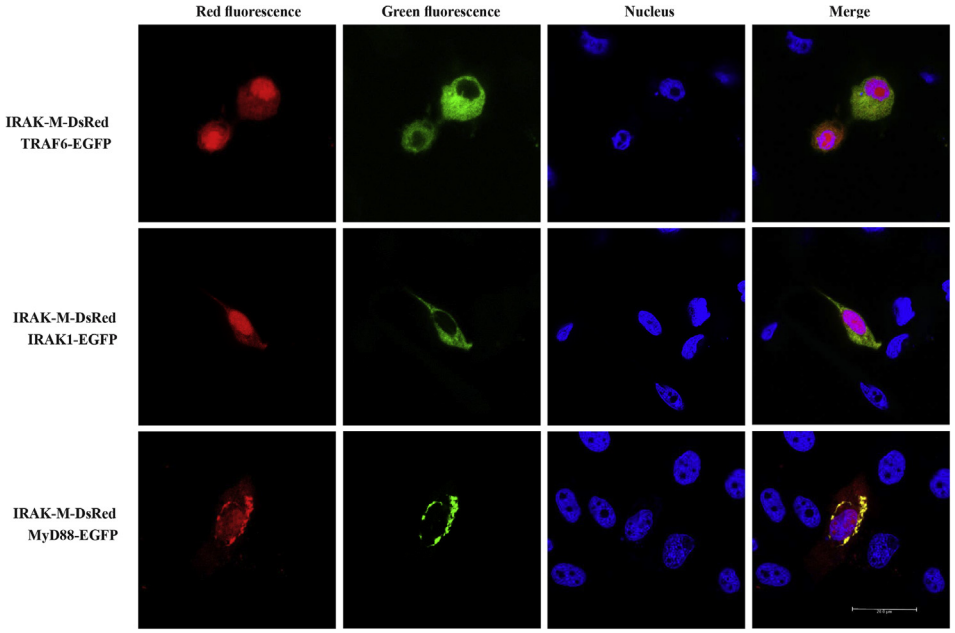

Fig. 7. Colocalisation of IRAK-M with related gene in CIK cells. Cells were transfected plasmids TRAF6-pEGFP, IRAK1-pEGFP, MyD88-pEGFP with IRAK-M-pDsRed, and fluorescence was observed at 24 h post-transfection. Green fluorescence showed the distribution EGFP-tagged proteins, red fluorescence showed the distribution of IRAK-M protein, and blue fluorescence showed the nucleus stained with Hoechst 33342 under a 63 × oil immersion objective lens (scale bar, 20 μm). (For interpretation of the references to colour in this figure legend, the reader is referred to the Web version of this article.)

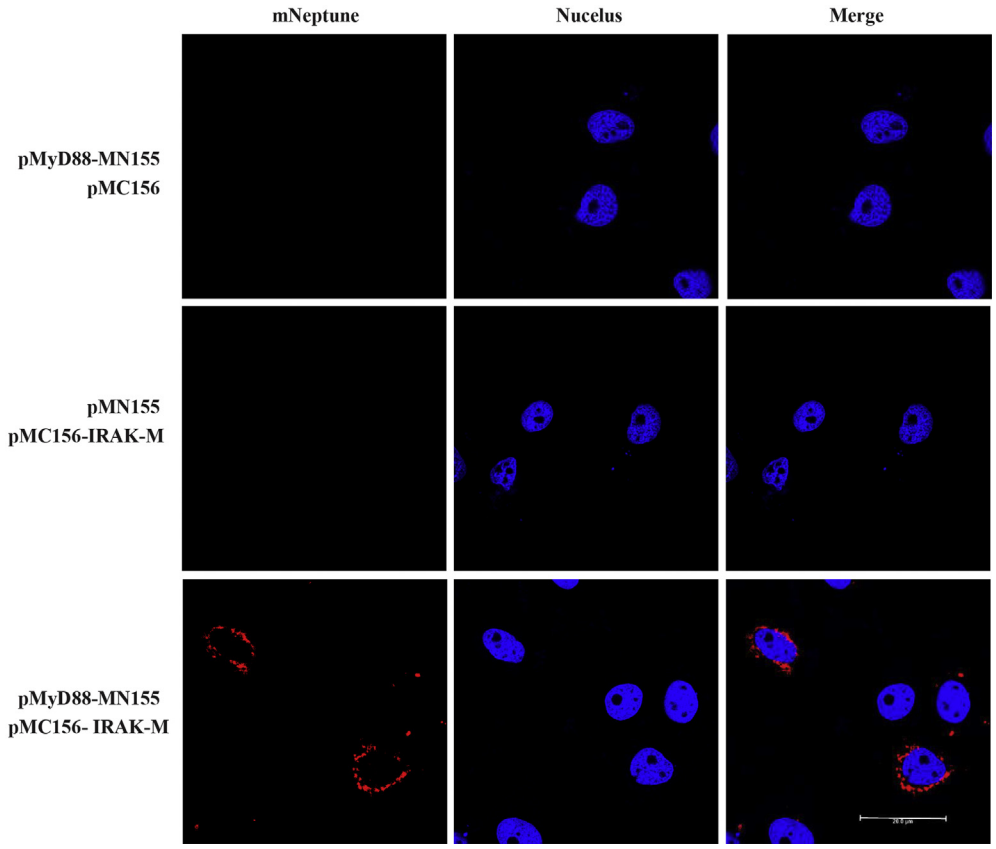

Fig. 8. Imaging of the protein-protein interaction by using far-red mNeptune-based BiFC in *vivo*. Plasmids pMyD88-MN155 and pMC156-IRAK-M were transfected into CIK cells alone or together. In the BiFC system, the fluorescence of the mNeptune channel was red, and the nucleus was stained with Hoechst 33342. The images were acquired using fluorescence microscopy and a 63 × oil immersion objective lens (scale bar, 20 μm). (For interpretation of the references to colour in this figure legend, the reader is referred to the Web version of this article.)

inflammatory cytokines. It is a pity that we did not get the antibody of IRAK-M, so the changes of IRAK-M protein in respond to GCRV or poly (I:C) could not be detected in the study. There are mounting evidences that NF-κB plays an important role in immune regulation system [43]. Hao Zhou found that IRAK-M was also able to interact with MyD88–IRAK-4 to form IRAK-M Myddosome to mediate TLR7-induced MEKK3-dependent second wave NF-κB activation [44]. In the present study, the same intriguing finding was also observed that the promoter activity of NF-κB could be activated by IRAK-M (Fig. 5).

TLRs were well known as the crucial roles for host to recognize and defense against pathogens in fish. Besides, more than 20 TLRs were detected in fish, including the orthologous to mammals (TLR1, 2, 3, 4, 5, 7, 8, and 9) and only existed in fish (TLR11, 12, 13, 14, 21, 22, and 23) [37,45]. IRAKs proteins have been identified as a vital regulator involved in TLRs signaling pathways via binding or dissociating with MyD88 and TRAF6 in mammals in recent years [4,6,and 7]. As mentioned previously, IRAK-M protein generally acts as a negative regulator of NF-κB activation in TLR signaling by its adaptor roles [22].

The subcellular localisation showed that IRAK-M protein was distributed uniformly throughout the entire cell. Interestingly, when co-transfected with MyD88, a remarkably bright signal occurred in the colocalisation of IRAK-M and MyD88 (Fig. 7), suggesting that MyD88 could recruit and relocate IRAK-M protein. To confirm this hypothesis, BiFC system was used to visualize the interaction of MyD88 with IRAK-M in CIK cells. Only co-transfection of pMyD88-MN155 and pMC156-IRAK-M could result in a bright red mNeptune fluorescence signal in the cytoplasm surrounding the cell nucleus (Fig. 8). Thus, the results further confirmed that IRAK-M interacted with MyD88 in CIK cells [4,11]. IRAK1/2-double deficient mice expresses significantly higher *IL-6* and *TNF-α* than that of IRAK1/2/M-triple deficient mice, together with our results suggest that IRAK-M is potential to become activated like other IRAK proteins and serve as a functional kinase [11,44].

In summary, the full-length cDNA of *IRAK-M* from grass carp was cloned and the transcriptional regulation pattern upon GCRV and poly (I:C) were described and discussed. Furthermore, among three crucial adaptor molecules, MyD88 protein was detected to recruit and interact with IRAK-M in CIK cells by subcellular localisation and BIFC system. Besides, deficient of IRAK-M in CIK cells with siRNA upregulated poly (I:C)-induced cytokines *IL-8*, *IL-6*, and *TNF-α*, which reveals that IRAK-M functions as a negative regulator of inflammatory cytokines. Our results demonstrate that *IRAK-M* gene plays an important role in innate immune regulation and will provide new insights into understanding the functional characteristics of the IRAK-M in teleosts.

Acknowledgments

This work was funded by the National Natural Science Foundation of China [grant number 31721005], the Hubei Natural Science Foundation of China [grant number 2015CFA007], the Strategic Pilot Science and Technology Projects (A) Category, Chinese Academy of Sciences [grant number XDA08030203], the National Natural Science Foundation of China [grant number 31702332], and the Hubei Natural Science Foundation of China [grant number 2017CFB374].

Appendix A. Supplementary data

Supplementary data to this article can be found online at https://doi.org/10.1016/j.fsi.2018.09.080.

References

[1] Y.W. Li, F. Zhao, Z.Q. Mo, X.C. Luo, A.X. Li, et al., Characterization, expression, and functional study of IRAK-1 from grouper, *Epinephelus coioides*, Fish Shellfish Immunol. 56 (2016) 374–381.
[2] R. Ahmad, P.K. Shihab, R. Thomas, M. Alghanim, A. Hasan, S. Sindhu, et al., Increased expression of the interleukin-1 receptor-associated kinase (IRAK)-1 is associated with adipose tissue inflammatory state in obesity, Diabetol. Metab. Syndrome 7 (2015) 71.
[3] M. Muzio, J. Ni, P. Feng, V.M. Dixit, IRAK (Pelle) family member IRAK-2 andMyD88 as proximal mediators of IL-1 signaling, Science 278 (5343) (1997) 1612–1615.
[4] A. Jain, S. Kaczanowska, E. Davila, IL-1 receptor-associated kinase signaling and its role in inflammation, cancer progression, and therapy resistance, Front. Immunol. 5 (2014) 553.
[5] A.G. Bowie, Insights from vaccinia virus into Toll-like receptor signalling proteins and their regulation by ubiquitin: role of IRAK-2, Biochem. Soc. Trans. 36 (3) (2008) 449–452.
[6] H. Cheng, T. Addona, H. Keshishian, et al., Regulation of IRAK-4 kinase activity via autophosphorylation within its activation loop, BBRC (Biochem. Biophys. Res. Commun.) 352 (3) (2007) 609–616.
[7] C. Kollewe, A.C. Mackensen, D. Neumann, et al., Sequential autophosphorylation steps in the interleukin-1 receptor-associated kinase-1 regulate its availability as an adapter in interleukin-1 signaling, J. Biol. Chem. 279 (7) (2004) 5227–5236.
[8] J. Brown, H. Wang, G.N. Hajishengallis, M. Martin, TLR-signaling networks: an integration of adaptor molecules, kinases, and cross-talk, J. Dent. Res. 90 (4) (2011) 417–427.
[9] T. Kawagoe, S. Sato, K. Matsushita, H. Kato, K. Matsui, Y. Kumagai, et al., Sequential control of toll-like receptor-dependent responses by IRAK1 and IRAK2, Nat. Immunol. 9 (6) (2008) 684–691.
[10] P. Cohen, Targeting protein kinases for the development of anti-inflammatory drugs, Curr. Opin. Cell Biol. 21 (2) (2009) 317–324.
[11] H. Wesche, X. Gao, X. Li, C.J. Kirschning, G.R. Stark, Z. Cao, IRAK-M is a novel member of the Pelle/interleukin-1 receptor-associated kinase (IRAK) family, J. Biol. Chem. 274 (27) (1999) 19403–1910.
[12] P. Escoll, C. del Fresno, L. Garcı'a, G. Vallés, M.J. Lendı'nez, F. Arnalich, E. LópezCollazo, Rapid up-regulation of IRAK-M expression following a second endotoxin challenge in human monocytes and in monocytes isolated from septic patients, Biochem. Biophys. Res. Commun. 311 (2) (2003) 465–472.
[13] W.J. Wiersinga, C. van't Veer, P.S. van den Pangaart, A.M. Dondorp, N.P. Day, S.J. Peacock, T. van der Poll, Immunosuppression associated with interleukin-1Rassociated-kinase-M upregulation predicts mortality in Gram-negative sepsis (melioidosis), Crit. Care Med. 37 (2) (2009) 569–576.
[14] L. Balaci, M.C. Spada, N. Olla, G. Sole, L. Loddo, F. Anedda, G. Pilia, IRAK-M is involved in the pathogenesis of early-onset persistent asthma, Am. J. Hum. Genet. 80 (6) (2007) 1103–1114.
[15] Q. Wu, D. Jiang, S. Smith, J. Thaikoottathil, R.J. Martin, R.P. Bowler, H.W. Chu, IL-13 dampens human airway epithelial innate immunity through induction of IL-1 receptor–associated kinase M, J. Allergy Clin. Immunol. 129 (3) (2012) 825–833.
[16] G.J. van der Windt, D.C. Blok, J.J. Hoogerwerf, A.J. Lammers, A.F. de Vos, C. van't Veer, T. van der Poll, Interleukin 1 receptor–associated kinase M impairs host defense during pneumococcal pneumonia, J. Infect. Dis. 205 (12) (2012) 1849–1857.
[17] M. Miyata, J.Y. Lee, S. Susuki-Miyata, W.Y. Wang, H. Xu, H. Kai, J.D. Li, Glucocorticoids suppress inflammation via the upregulation of negative regulator IRAK-M, Nat. Commun. 6 (2015) 6062.
[18] M. Lech, C. Kantner, O.P. Kulkarni, M. Ryu, E. Vlasova, J. Heesemann, H.J. Anders, Interleukin-1 receptor-associated kinase-M suppresses systemic lupus erythematosus, Ann. Rheum. Dis. 70 (12) (2011) 2207–2217.
[19] M. Berglund, S. Melgar, K.S. Kobayashi, R.A. Flavell, E.H. Hörnquist, O.H. Hultgren, IL-1 receptor-associated kinase M downregulates DSS-induced colitis, Inflamm. Bowel Dis. 16 (10) (2010) 1778–1786.
[20] T.J. Standiford, R. Kuick, U. Bhan, J. Chen, M. Newstead, V.G. Keshamouni, TGFb-induced IRAK-M expression in tumor-associated macrophages regulates lung tumor growth, Oncogene 30 (21) (2011) 2475–2484.
[21] P. Jin, L. Bo, Y. Liu, W. Lu, S. Lin, et al., Activator protein 1 promotes the transcriptional activation of IRAK-M, Biomed. Pharmacother. 83 (2016) 1212–1219.
[22] W. Chen, A. Saxena, N. Li, J. Sun, A. Gupta, D.W. Lee, et al., Endogenous IRAKM attenuates postinfarction remodeling through effects on macrophages and fibroblasts, Arterioscler. Thromb. Vasc. Biol. 32 (11) (2012) 2598–2608.
[23] F.C. del, K. Otero, L. Gomez-Garcia, M.C. Gonzalez-Leon, L. Soler-Ranger, P. FuentesPrior, et al., Tumor cells deactivate human monocytes by up-regulating IL-1 receptor associated kinase-M expression via CD44 and TLR4, J. Immunol. 174 (5) (2005) 3032–3040.
[24] A. Soares-Schanoski, T. Jurado, R. Cordoba, M. Siliceo, C.D. Fresno, V. Gomez-Pina, et al., Impaired antigen presentation and potent phagocytic activity identifying tumor-tolerant human monocytes, Biochem. Biophys. Res. Commun. 423 (2) (2012) 331–337.
[25] Q. Tan, M. Majewska-Szczepanik, X. Zhang, et al., IRAK-M deficiency promotes the development of T1DM in NOD mice, Diabetes 63 (8) (2014) 2761.
[26] P.R. Rauta, M. Samanta, H.R. Dash, B. Nayak, S. Das, Toll-like receptors (TLRs) in aquatic animals: signaling pathways, expressions and immune responses, Immunol. Lett. 158 (2014) 14–24.
[27] X. Zhao, X. Hong, R. Chen, L. Yuan, J. Zha, et al., New cytokines and TLR pathway signaling molecules in Chinese rare minnow (*Gobiocypris rarus*): molecular characterization, basal expression, and their response to chlorpyrifos, Chemosphere 199 (2018) 26–34.
[28] Y. Xu, Y. Huang, S. Cai, Characterization and function analysis of interleukin-1 receptor-associated kinase-1 (IRAK-1) from Fenneropenaeus penicillatus, Fish Shellfish Immunol. 61 (2017) 111–119.
[29] R. Huang, J. Lv, D. Luo, et al., Identification, characterization and the interaction of Tollip and IRAK-1 in grass carp (Ctenopharyngodon idellus), Fish Shellfish Immunol. 33 (3) (2012) 459–467.
[30] Y.W. Li, X.B. Mo, L. Zhou, et al., Identification of IRAK-4 in grouper (Epinephelus coioides) that impairs MyD88-dependent NF-κB activation, Dev. Comp. Immunol. 45 (1) (2014) 190–197.
[31] Y. Liu, S. Yu, Y. Chai, et al., Lipopolysaccharide-induced gene expression of interleukin-1 receptor-associated kinase 4 and interleukin-1β in roughskin sculpin (Trachidermus fasciatus), Fish Shellfish Immunol. 33 (4) (2012) 690–698.
[32] Y. Yu, Q. Zhong, C. Li, et al., Identification and characterization of IL-1 receptor-associated kinase-4 (IRAK-4) in half-smooth tongue sole Cynoglossus semilaevis, Fish Shellfish Immunol. 32 (4) (2012) 609–615.
[33] P.E. Phelan, M.T. Mellon, C.H. Kim, Functional characterization of full-length TLR3, IRAK-4, and TRAF6 in zebrafish (Danio rerio), Mol. Immunol. 42 (9) (2005) 1057–1071.
[34] P. Chu, L. He, L. Xiong, et al., Molecular cloning, expression analysis and localization pattern of the MST family in grass carp (*Ctenopharyngodon idella*), Fish Shellfish Immunol. 76 (2018) 316–323.
[35] Y. Wang, Y. Lu, Y. Zhang, et al., The draft genome of the grass carp (*Ctenopharyngodon idellus*) provides insights into its evolution and vegetarian adaptation, Nat. Genet. 47 (6) (2015) 625–631.
[36] K.J. Livak, T.D. Schmittgen, Analysis of relative gene expression data using real-time quantitative PCR and the $2^{-\triangle\triangle Ct}$ method, Methods 25 (4) (2001) 402–408.
[37] Y. Rao, J. Su, Insights into the antiviral immunity against grass carp (*Ctenopharyngodon idella*) reovirus (GCRV) in grass carp, J. Immunol. Res. 2015 (2015) 670437.
[38] Y. Palti, Toll-like receptors in bony fish: from genomics to function, Dev. Comp. Immunol. 35 (12) (2011) 1263–1272.
[39] M.K. Purcell, K.D. Smith, L. Hood, J.R. Winton, J.C. Roach, Conservation of toll-like

receptor signaling pathways in teleost fish, Comp. Biochem. Physiol. Genom. Proteonomics 1 (1) (2006) 77–88.
[40] O. Rosati, M.U. Martin, Identification and characterisation of murine IRAK-M, Biochem. Biophys. Res. Commun. 293 (2003) 1472–1478.
[41] Q. Huang, D. Xie, H. Mao, et al., *Ctenopharyngodon idella* p53 mediates between *NF-κB* and *PKR* at the transcriptional level, Fish Shellfish Immunol. 69 (2017) 258–264.
[42] P. Chu, L. He, Y. Li, et al., Molecular cloning and functional characterisation of *NLRX1* in grass carp (*Ctenopharyngodon idella*), Fish Shellfish Immunol. 81 (2018) 276–283.
[43] Q. Li, Inder M. Verma, NF-κB regulation in the immune system, Nat. Rev. Immunol. 2 (2002) 725–734.
[44] H. Zhou, M. Yu, K. Fukuda, J. Im, P. Yao, et al., IRAK-M mediates Toll-like receptor/IL-1R-induced NF-κB activation and cytokine production, EMBO J. 32 (2013) 583–596.
[45] Y. Palti, Toll-like receptors in bony fish: from genomics to function, Dev. Comp. Immunol. 35 (12) (2011) 1263–1272.